Coupled Mode Theory and 50/50 Splitter

Eduardo A. V. Souza, RA: 250950
"Gleb Wataghin" Institute of Physics
UNICAMP
Campinas, Brazil

Ivan Prearo (RA 237215)
"Gleb Wataghin" Institute of Physics
UNICAMP
Campinas, Brazil

Abstract—In this work, we aimed to design a 50/50 splitter made a two-waveguide coupled system. First, we started with a pre-analysis with COMSOL to optimize the material of the waveguides, their width and thickness, alongside with a resonable gap to obtain a short in length splitter. At the end, we analysed two cases of beamplitter, the first with identical waveguides, and the second with one waveguide with doubled dimensions. We found that the second case is better to obtain a more compact splitter.

Index Terms—Waveguides, Coupled Mode Theory, Beamsplitter.

I. INTRODUCTION

In this section, we aim to describe the investigation to choose the material and the geometrical parameters of the waveguides belonging the coupled system. In the first place, we considered SiO_2, TiO_2, Si_3N_4, and Ag_3AsS_3 as the possible materials due to their renowed applications in photonic integrated circuits (PIC). Fig. 1 displays the dispersion of each one of these materials. As it is evident, Ag_3AsS_3 has the greatest values of refravice index (RI) and SiO_2 has the lowest, while TiO_2 and Si_3N_4 are intermediate cases.
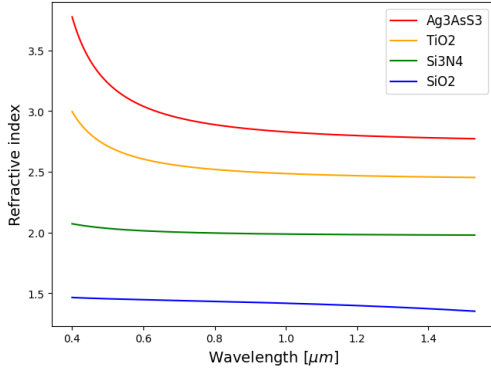

Fig. 1: Dispersion relation for the SiO_2, TiO_2, Si_3N_4, and Ag_3AsS_3.

Motivated by the common use of SiO_2 and TiO_2 in waveguides, and the info they present distinctive dispersion relations, TiO_2 presenting the highest values, we will focus on these materials as the candidates for the beam splitter. So, their dispersion relations are described by Eq. (1).

$$n_{SiO_2} = \sqrt{1 + \frac{0.6961663\lambda^2}{\lambda^2 - 0.0684043^2} + \frac{0.4079426\lambda^2}{\lambda^2 - 0.1162414^2} + \frac{0.8974794\lambda^2}{\lambda^2 - 9.896161}} \quad (1a)$$

$$n_{TiO_2} = \sqrt{5.913 + \frac{0.2441}{\lambda^2 - 0.0803}} \quad (1b)$$

To understand the number of modes in a waveguide, we plotted the characteristic equations for SiO_2 for the infinite dielectric slab case, which has a easier mathematical description. The generic characteristic equation is described by Eq. (2) where d is the thickness of the slab, and the plot of the functions describing this equation, f_1 and f_2, are plotted in Fig. 3.

$$f_1(\sin(\theta)) \equiv \tan\left[\pi\left(\frac{\sin(\theta)d}{\lambda} - \frac{m}{2}\right)\right]$$
$$= \sqrt{\frac{\sin^2(\overline{\theta}_c)}{\sin^2(\theta)} - 1} \equiv f_2(\sin(\theta)) \quad (2)$$
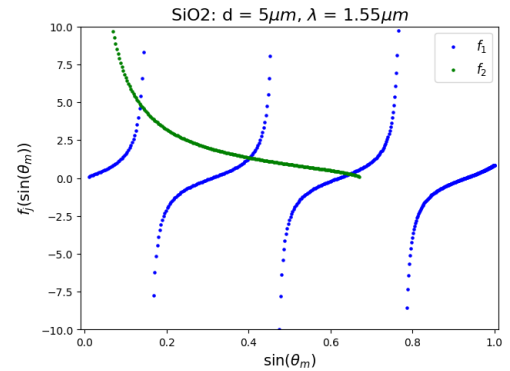

Fig. 2: SiO_2.

Fig. 3: Plot of the characteristic equations for the SiO_2 and TiO_2 infinite slab case.

From Fig. 3 it is evident f_1 and f_2 intersect at three points, that is, this waveguide presents only three modes. As we increase the thickness of the slab, we make room for more

modes to appear. As the next step, we plotted the characteristic functions for the rectangular dielectric case for SiO_2 and TiO_2, considering the approximation $E(x, y) = X(x)Y(y)$. Considering these components independent, we can solve the characteristic equation for x and y dimensions separately, find θ_{mx} and θ_{my}, and latter on combine into the solution described by Eq. (3) where $k_j = n_1 k_0 \sin(\theta_{m_j})$, $\forall j \in \{1, 2\}$.

$$\beta_{m_x, m_y} = \sqrt{(n_1 k_0)^2 - k_x^2 - k_y^2} \qquad (3)$$

With the results above, we could note the waveguide made of SiO_2 presented a smaller number of modes when compared to the TiO_2 case. Since in this work we are concerned with a waveguide with a few guided modes only, we decided to explore the coupled system made of SiO_2 cores and the geometrical parameters $t_{core,j} = 2\mu m$, (i) $w_{core,j} = 6\mu m$, and (ii) $w_{core,2} = 2w_{core,1} = 6\mu m$ and $t_{core,j} = 2\mu m$. Another observation, is that we are considering the two cores for the coupled systems to be aligned at the center of the cartesian coordinate system, in a sense the gap in the y-direction is $d_y = 0$, otherwise it would distort the overlapping region and would not give much different information. Thus, we can name the gap in the x-direction simply d.

II. 50/50 SPLITTER

In this section, we aim to effectively model the 50/50 splitter describe at the end of Sec. I with COMSOL with the cores made by SiO_2 and the cladding made of air with the following geometrical parameters $t_{clad} = 15\mu m$ and $w_{clad} = 30\mu m$. So, we discuss the case of two identical cores with $t_{core} = 2\mu m$ and $w_{core} = 6\mu mu$ in Subsec. II-A and in Subsec. II-B we analyse what changes if we let the first core to have width $w_{core,1} = w_{core,2}/2 = 3\mu m$, that is, core 2 presents the double width of core 1.

A. Identical cores

For this subsection and the following, it is important to note we are considering $1.55\mu m$ as the reference input wavelength due its huge applicability in telecommunication and just the first even and odd supermodes. Also, we are separating the even supermodes from the odd ones based on the arrow surface plot of $\mathbf{E}_x$ vs. $\mathbf{E}_y$ onto the surface plot of $\|\mathbf{E}\|$ as indicated in Fig. 4. The even modes present arrows in the same direction for both cores, and the odd present arrows in the opposite direction.
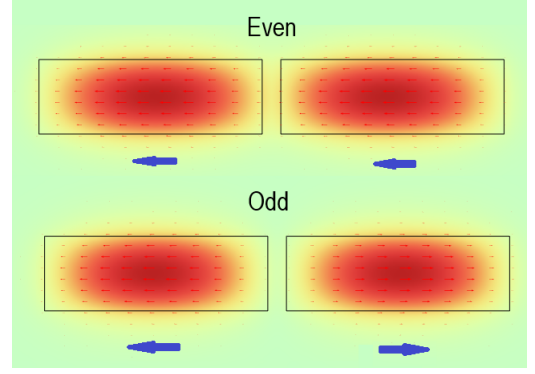

Fig. 4: Distinction between even and odd supermodes SiO_2 core with $w_{core,j} = 6\mu m$ and $t_{core,j} = 2\mu m$, and the gap between cores given by $d = 0.5\mu m$.

We varied the gap between the cores and decided to use $d = 0.5 mum$ due its considerable overlapping region and because lower gaps might be difficult to fabricate with techniques such as photolitography.

Furthermore, calculate the butt coupling, inter-mode and auto-phase-shift coefficients by simulation the individual guides (just one core and the cladding) and separating them into studies in COMSOL. For those values which presented imagnary part, we noticed the real part is much greater, so in Tab. III we put only the absolute value of the real component.

$m_1 \to m_2$	$|\Re(C_{12})|$	$|\chi_{11}|[m^{-1}]$	$|\Re(\kappa_{12})|[m^{-1}]$
$0 \to 0$	0.0073	$1.0890 \cdot 10^5$	3366.5
$0 \to 1$	$2.2582 \cdot 10^{-7}$	$1.0890 \cdot 10^5$	0.5
$0 \to 2$	0.0154	$1.0890 \cdot 10^5$	7207.3

TABLE I: Butt coupling, inter-mode and auto-phase-shift coefficients for different individual guide modes.

Aiming to explore the sensitivity of this splitter with the wavelength, we repeated the simulation for the range $\lambda \in [1.40\mu m, 1.70\mu m]$ and obtained from COMSOL the effective refractive index n_{eff} for each supermode. Using $\beta = k_0 n_{eff}$, we could obtain the propagation constant for each supermode mode as well.

Once we now the order of the even and odd supermodes for a given wavelength, we can compute the coupling length L_c, the length needed for the light being initally guided through the first core to be entirely coupled into the second core. To do so, we used Eq. (4), where $\Delta\beta \equiv \beta_{even} - \beta_{odd}$. These values are place in Tab. II, which also displays the coupling efficiency η from the first core into the second one considering a intercation length of $L_{int} = 484.4\mu m$.

$$L_c = \frac{\pi}{\Delta\beta} \qquad (4)$$

$\lambda[\mu m]$	L_c	$\eta[\%]$
1.40	1400.0	34.6
1.45	1450.0	33.4
1.50	1071.4	45.2
1.55	968.7	50.0
1.60	888.9	54.5
1.65	750.0	64.59
1.70	653.8	74.09

TABLE II: Coupling length and coupling efficiency coefficient for the first supermode making $L_{int} = 484.4\mu m$ varying the input wavelength for the identical cores.

As you can see from the table above, the operational range of this 50/50 beamplitter is short, it can operate within a 5% margin of η in the range $\lambda \in [1.50\mu m, 1.60\mu m]$, a span of $100nm$ only. Also, if we cconsider a fabrication error in the interation length of 10%, we would have a coupling interval in $1.55\mu m$ of $\eta \in [45\%, 55\%]$.

B. First core with half width

For the case of the first core to present half the widht of the second, we repeated the same analysis of Subsec. II-A.

$m_1 \rightarrow m_2$	$|\Re(C_{12})|$	$|\chi_{11}|[m^{-1}]$	$|\Re(\kappa_{12})|[m^{-1}]$
$0 \rightarrow 0$	0.0169	$1.6146 \cdot 10^5$	6830
$0 \rightarrow 1$	$1.6100 \cdot 10^{-6}$	$1.6146 \cdot 10^5$	2
$0 \rightarrow 2$	$4.0358 \cdot 10^{-6}$	$1.6146 \cdot 10^5$	3

TABLE III: Butt coupling, inter-mode and auto-phase-shift coefficients for different individual guide modes.

The wavelength sensitivity is analysed in Tab. IV. As you can see, the η vary much less with the wavelength than the previous case. For the range $\lambda \in [1.40\mu m, 1.70\mu m]$, a span of $300nm$, η has a margin less than 2%. Thus, if we accept a margin of 5%, we could extend even further the wavelength range. Again, if we consider a fabrication error in the interaction length of 10% for $1.55\mu m$ input wavelength, we would obtain a efficiency interval of $[45\%, 55\%]$. In this case, the interaction length error would contribute more to the deviation of the 50/50 coupling when compared to the wavelength variation.

$\lambda[\mu m]$	L_c	$\eta[\%]$
1.40	179.5	49.1
1.45	176.8	49.8
1.50	174.4	50.5
1.55	176.1	50.0
1.60	170.2	51.8
1.65	175.5	50.2
1.70	177.1	49.7

TABLE IV: Coupling length and coupling efficiency coefficient for the first supermode making $L_{int} = 88.1\mu m$ varying the input wavelength for different size cores.

III. Conclusion

In summary, we began our study with a investigation of the material of cores for the coupled system, their geometry and the gap distance between them. At last, we projected two cases of a 50/50 beamplitter varying the geometry of the cores, and analyse their sensitivity with the wavelength and the length interaction error.

Appendix

Rewriting of the curl of a scalar function depending only on z multiplied by a vector function:

$$\nabla \times \left(a_{(z)}\vec{v}\right) = a_{(z)}\nabla \times \vec{v} + \nabla a_{(z)} \times \vec{v} = a_{(z)}\nabla \times \vec{v} + \frac{da_{(z)}}{dz}\hat{z} \times \vec{v} \quad (5)$$

Cross and dot products of vectors of the type $\vec{A}e^{j\phi_1}$ e $\vec{B}e^{-j\phi_2}$

$$\begin{cases} \vec{A}e^{j\phi_1} \times \vec{B}e^{-j\phi_2} = (\vec{A} \times \vec{B})e^{j(\phi_1 - \phi_2)} \\ \vec{A}e^{j\phi_1} \cdot \vec{B}e^{-j\phi_2} = (\vec{A} \cdot \vec{B})e^{j(\phi_1 - \phi_2)} \end{cases} \quad (6)$$